

Chapter II

Hardware and Software setup

2.1 Experimental Setup

In our home build subpicosecond pump-probe microscope (PPM) we started with an empty optical tabletop and planned to build a versatile highly customizable optical layout from the oscillator to the inverted microscope. The complete layout is shown in figure 1. Starting from our laser source, Coherent Chameleon (700-1040 nm , 80MHz) is fed to Coherent Compact OPO to generate the pump or the probe beam based on the experimental setup. The bypass of the OPO serves as the probe(green line) and the output of the OPO serves as the pump beam(red line). For ease of alignment and a better control over the beam paths, it is best to bring both beam height to match the side input height of the microscope (Eclipse TE2000-U, Nikon). For the OPO output, we setup a doubling BBO crystal depending on the experiment. After adjust the height we will keep the same height throughout the layout for consistency and ease of troubleshooting. There is a need to synchronize the oscillator and OPO output as the beam inside OPO cavity passes a longer length (around 2m). This synchronization path is not shown in figure 1 for clarity reasons. The two out put are measured for

polarization contrast right out side of output aperture. This matter will be discussed later in details, however, it is an important measurement for several reasons; 1) the attenuation is controlled with a half-wave plate and polarization pair; 2) p-polarized beam is essential to get output with the best modulation depth from the AOM; 3) vortex phase plate (VPP) is sensitive to polarization for its optimum operation; 4) mixing the two pumps is done with a polarization beam splitter. In our case the polarization contrast was very poor for the fundamental. It showed some wavelength dependencies as well. Based on the user manual of this oscillator this parameter should be 500:1 but our measurement was only 20:1 which is very different from the specification. It is best to correct the polarization at this point to have better control over the polarization rotation over the rest of the layout. To do this, a Glan-Taylor polarizer was used to set the p polarization.

After having the height right and the polarization right, it is best to align the delay stage of the probe. The delay stage has 300 mm travel during which the beam pointing should remain the same. On the delay line a silver coated halo-type retroreflector is installed. This element (Figure 2) contains three mirrors and guarantees the output beam is parallel to the input beam regardless of the incident angle [19]. Therefor the best practice here is, to align the input beam in-line with the delay line. To achieve high precision during this step the reflected beam should be guided and projected on a target as far as possible; mark this position. By moving the delay stage back and forth, and adjust paired mirror that controls the

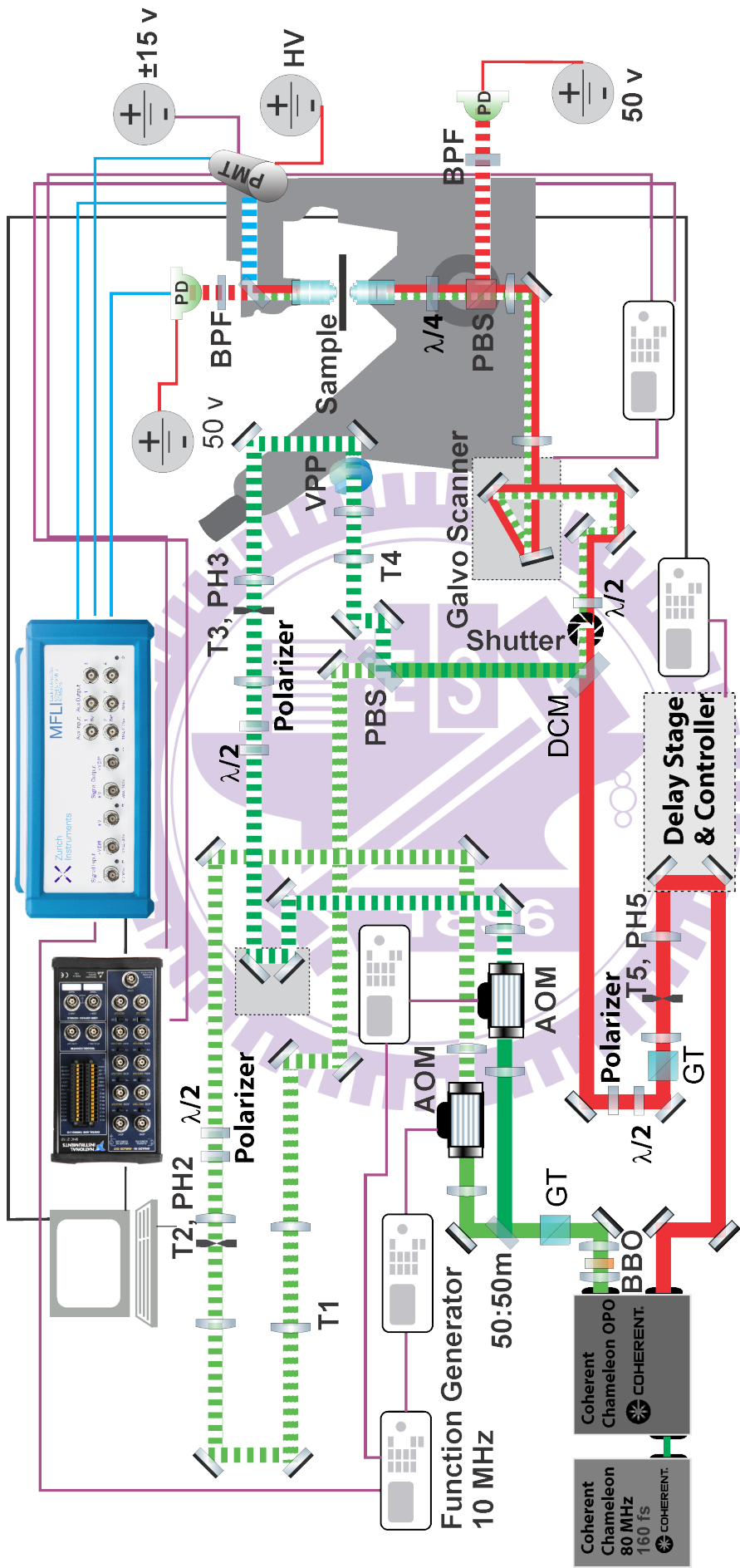


Figure 1: The detailed schematic of sub-picosecond Sub-Diffraction pump-probe microscope. Two pumps are modulated with 180° phase difference at 10 MHz. 50:50 is a beam splitter. $\lambda/2$: halfwave plate; PH: pinhole; HV: High Voltage power supply; T: Telescope; BPF: bandpass filter; PBS: Polarization beam splitter; VPP: vortex phase plate; GT: Glan-Taylor polarizer; DCM: dichroic mirror.

pointing of the incident beam. This routine should be repeated till the beam on the target does not move by moving the stage which indicates a well aligned beam. This step is crucial to the rest of the setup. Therefore, It is advised this step is carried with patience and precision to have consistent data and alignment procedure. If beam pointing changes when the delay line moves, it will deteriorate all the alignment after the retroreflector and even a slight deviation can cause wrong decay profile. It is noticeable that the polarization after the retroreflector is rotated and partially depolarized there measures should be taken to filter and correct the polarization. [20]

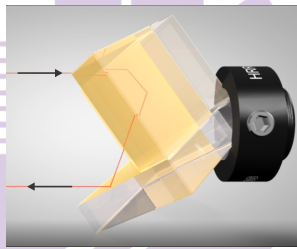


Figure 2: Retroreflector. The output beam is always parallel to the input beam.

In this setup we use a pair of galvo scanners to rasterize the field of view. The mirrors connected to these scanners can accept maximum 2 mm beam size. Keeping that in mind, with the fact that the beam path is long we need to make sure the input beam size does not exceed this value. To ensure this we need two telescopes on each path to first expand and then shrink the beam size. In addition to the size limit of the scanning mirrors, this configuration allows us to be able to overfill the aperture of the objective to obtain diffraction limit spot size. In addition to these telescopes, in the pump beam path there are another sets for the AOM configuration.

There are two ways to build the telescope; a pair of negative and positive lenses or a pair of positive lenses. Both have their advantages which will be discussed later. Briefly, The positive-negative pair configuration is more compact and less chromatic aberration, the use of two positive lens enables us to setup of pinhole as a spatial filter. In each of the three beam paths there is a pinhole to clean-up the beam mode .

At this, we need to setup the VPP to generate toroidal laser mode. To obtain this, the beam size should be expanded to fill the area on the dedicated region on the VPP (5mm). This phase plate, is made for an array of various wavelengths which imposes a limitation on the pump beam wavelength selection. To optimize the toroidal mode generation one can observe the transient beam on a white card while adjusting the position and tilt angle of the VPP.

Now it is time to combine all the three beams and guide them to the galvo-scanners. To combine the two pumps a polarization beam splitter (PBS) is used. The polarization of the the pump beams should be set one in p and one in s direction so this configuration can be used. Using a PBS is better than using other methods, such as using a 50:50 mirror, to combine two beams with the same wavelength, as there is no intensity loss. The next step is to combine the two beams with the probe beam which is done with a dichroic mirror.

Now that all the beams are colinearly lined up, it is best that we roughly synchronize the laser pulses. To do so, we put a fast photodiode(DET10A, Thorlabs), after the last dichroic mirror and connect it to an oscilloscope

(TDS3032B, Tektronix). The oscilloscope should be triggered with the sync out of the Coherent Chameleon as a reference. In Figure 1 there are two delay lines which is necessary to bring the three beams in sync. In case the beams are very separated (more than 100 ps) in time domain, the beam path itself should be adjusted to compensate for delays rather than moving the delay line. After the beams are relatively synchronized a selection of samples and sources of signals (SRS signal from cooking oil) can be used to find the precise time-zero.

The beam now is ready to be scanned and passed through the scan lens, tube lens, objective lens, condenser lens and to the detector. This beam path requires precise alignment that I will go through step by step. First the scanning mirrors should be set to their default position from the driver. then with a help of a large pinhole placed at the left port of the microscope we try to manually adjust the beam in x and y to be in the center of the pinhole. Then the scan lens is installed and positioned in a way that when the mirrors are scanning the beam at the back aperture of the objective plane does minimum movement with the minimum distortion. The beam need alignment along the objective and condenser lens as well. To do so, the scanning mirrors are set to default position. Then our designed alignment tool (Figure 3) is placed at two positions, at the objective mount and 40 cm (or even more) away from it. For the later position, we use the lens tube system from Thorlabs attached to the objective lens mount. By walking the two mirrors before the scanner and switching the alignment tool between these two positions one should be able to obtain a precise

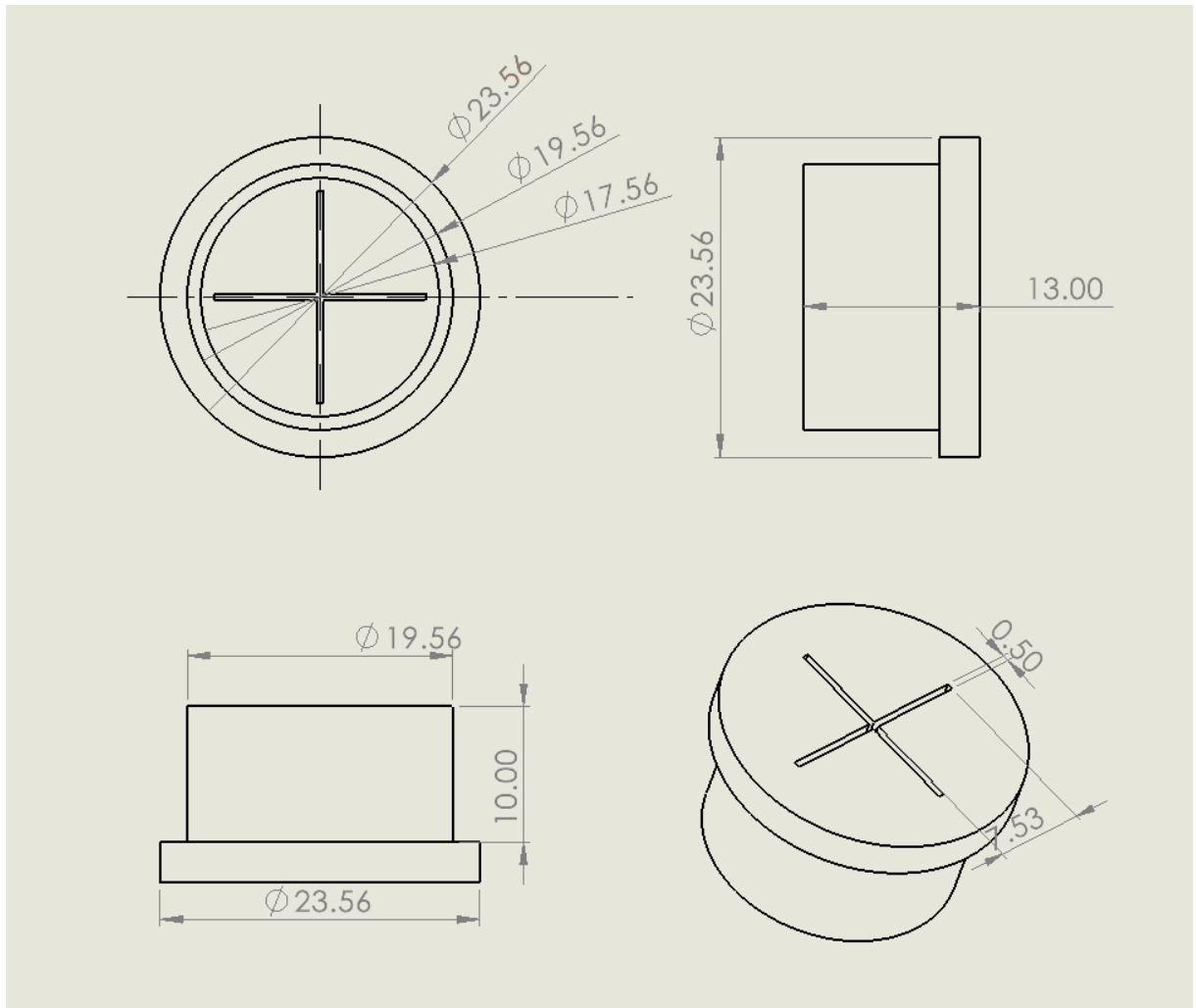


Figure 3: Drawing of the alignment tool for RMS system. All the numbers are in millimeters.

alignment vertically. After this step it is better to mark the laser spot on top of the microscope if possible for easier alignment in the future.

As a note, as the beam path is long to accommodate many optical elements, laser modulator and path length compensation, all the lenses and mirrors (as much as possible) here are achromatic and dielectric respectively.

2.2 Detailed Alignment Procedures

During building the Pump probe microscope (PPM), we faced a series of technical challenges that are basically caused by the nature of optical components and electronics circuitry. Overcoming these obstacles gave us a deeper insight of the instrument and helped to get faster in alignment optimization, better SNR and more precision in overall. In this section each optical or electro-optical is discussed with its brief specifications, alignment procedure, its effect on beam quality and how to compensate for it.

2.2.1 AOM Alignment and Optimization

acousto-optic modulator (AOM) (Figure 4) is an optical element that is used internally or externally to have control over the intensity or direction of the laser beam; it is referred to as modulation for intensity variation and deflection for the direction change. The acoustic wave inside the medium generates a local grating by means generating a sinusoidal refractive index wave. This local grating diffracts the input beam in several orders. 0_{th} Order is in the same direction as the input beam and contains unmodulated beam as an offset. The 1_{st} order has the highest efficiency with no offset with proper alignment of the incident angle between the laser light and the direction in which the acoustic wave propagate in the medium. The angle between the 0_{th} and 1^{st} order is defined as:

$$\theta = \frac{\lambda f_a}{V_a} = 2\theta_b \quad (1)$$

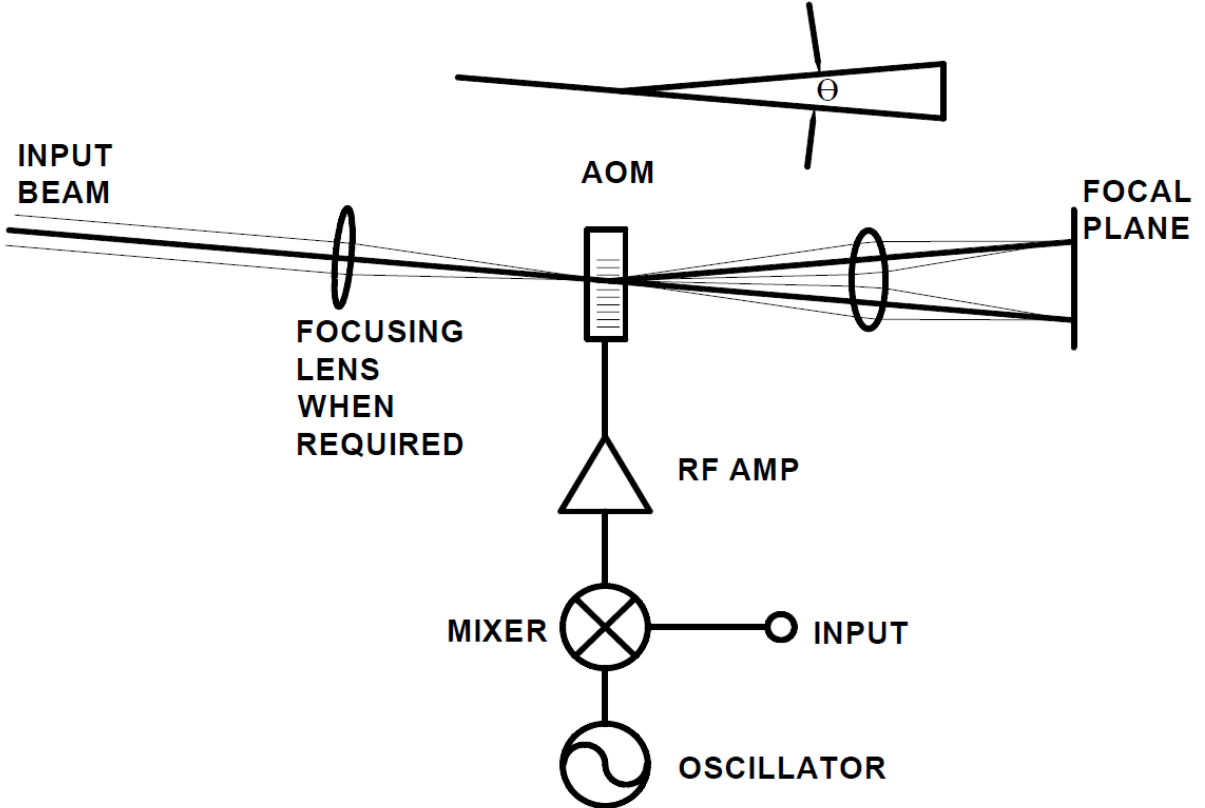


Figure 4: A typical AOM schematic that can modulate the input input beam at high frequencies. θ is the deflection angel.

Where λ is the wavelength, V_a is the acoustical velocity of the material, f_a is the acoustic frequency, θ_b is the brag angel. [21]

In Figure 5 a comparison between 1st order modulation depth and 0th order with low and optimized modulation depth is presented. While having low modulation, required intensity to obtain the same order of signal compared to the optimized condition, should be higher so the modulated part of the beam reaches the same order which also may result in having a higher DC (unmodulated beam) that can cause photo-degradation to the sample. The DC portion of the beam does not contribute to the signal in a heterodyne detection scheme. Therefore, having a higher amplitude for the modulated part of the beam is vital to avoid damages to the sample

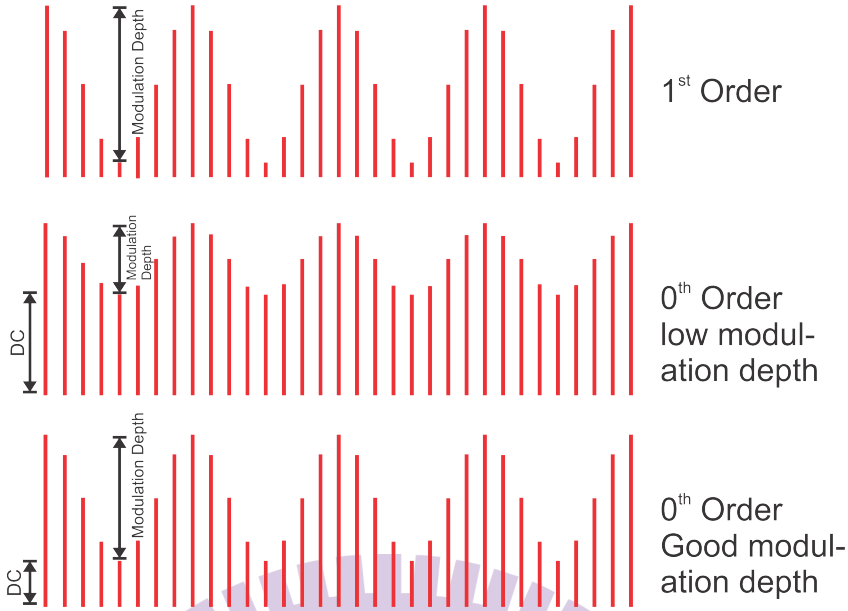


Figure 5: A schematic illustration of 1st and 0th order modulation depth comparison.

and consistent result during measurement.

The AOM In our setup was Gooch and Haousego 1080-197 for near IR and 1080-125 for visible region. Here we discuss the steps and measurements necessary to optimize this optical element and obtain the highest conversion efficiency¹.

During setting up the layout, it was found that the AOM ouput has a very low modulation depth and high background if not setup properly. The conversion efficiency could reach $\approx 89\%$ (when done carefully) when the device is driven from the front-panel of the function generator (DS345, Standford Research System ²) which there is full control over the wave form, amplitude and DC offset. Using the front panel series of measurements were done to compare how different parameters affect the conversion efficiency.

¹Conversion efficiency is defined by the ratio modulation depth over the maximum in voltage.

²later we switched to GW Instek MFG-2260MFA function generator

- Wave form (Sinusoidal or Square):

Square wave could affect the conversion efficiency and changing to sinusoidal cause the efficiency drop to $\approx 80\%$ from $\approx 89\%$. This can be explained by assuming the crystal responses better to sharp rise of a square wave rather than the gradual rise of the sinusoidal wave. In our current scenario the rise time of the AOM crystal is 25 ns therefore to have better conversion efficiency the rise time of the driving modulation should be smaller than this value. It is noticeable that the back-panel of DS34 output is only limited to sine wave.

- Wave amplitude:

Base on the manual the crystal is tested under the $V_{pp}=1$ while regarding our observations by varying the wave amplitude we observed lower conversion efficiency for values $V_{pp} \leq 1$ and for values above 1 volts there was no significant changes. Knowing this, the back-panel output suffers from its amplitude being around 0.9 volts.

- DC offset:

In this case having a wave varying from 0 to 1 shows more stable results compared to -0.5 to +0.5 mode while it also guarantees the 0th beam path remains intact compare to the original beam path while the AOM is off. It is also important

to bear in mind that the back-panel output only delivers amplitude modulation from -0.5 to +0.5.

These through examination helped us to design a DC level shifter by means of a high-speed op-amp (THS3202EVM) so that one can use a DS345 function generator to drive two AOMs synchronously. This configuration allows one to have control over the relative phase between the two output as well. The only limitation is the fixed frequency (10 MHz) which is limited by ouput in the back panel of this instrument.

Knowing the factors above, we decided to find a starting point for setting up the AOM from the driver side. The driver of this device can envelope the input modulation signal at 80 MHz and generate an radio frequency (RF) wave accordingly. This RF wave is then converted to acoustice wave at the peizo stage inside the crystal chamber. To get a better understanding how these RF is envelopin the input frequency we connected the driver output to an oscilloscope to monitor the enveloped signal and tune the input signal parameters, such as waveform, duty-cycle, phase, amplitude and offset. Doing this, we can find a good starting point without monitoring the laser output off the AOM. Shown in the Figure 6, is the a well optimize enveloped signal that is ready to be sent to the AOM module. What we are looking for is an waveform enveloped with the internal clock of the AOM driver that resembles the square wave (or any arbitrary waveform if required) output of the function generator.

Although the aforementioned starting point is fairly results in a high conversion ratio, it is best to optimize one more step further by monitoring

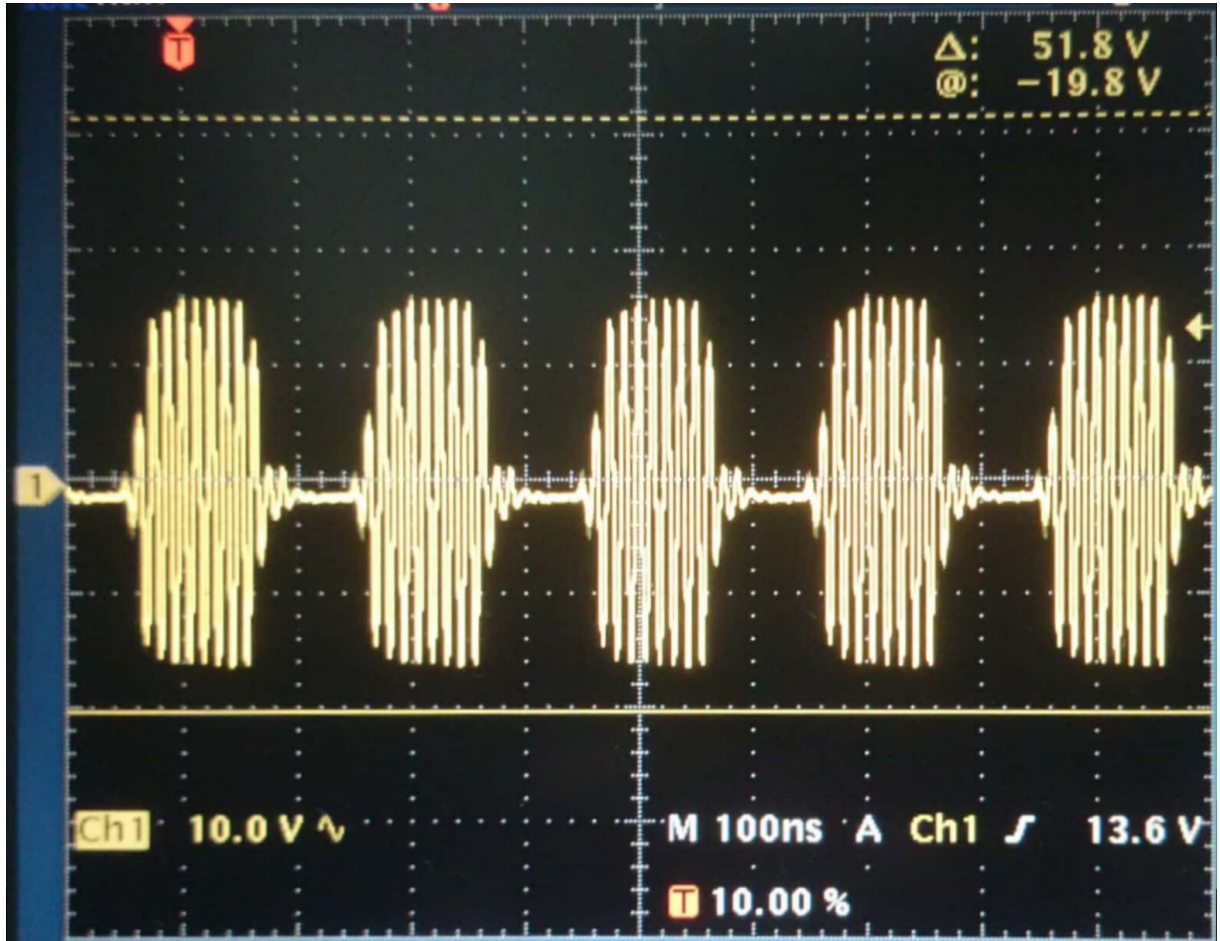


Figure 6: A well-enveloped modulation signal with the input clock of the AOM driver.

the beam output after the AOM. To do so, a fast photodiode (DET10A2, Thorlabs) is placed after the AOM. The beam is guided so the 1st order beam enters the detector. We then monitor the modulated laser beam on the oscilloscope. A typical bad modulation is shown in Figure 7. It is shown that there is still some residual beam appear as unmodulated at 1_{st} order output. It is possible though to achieve a better modulation result by fine tuning the level of DC offset and amplitude of the waveform on the function generator. After minor fine tuning one is able to get a perfect modulation with no unmodulated signal (Figure 8).

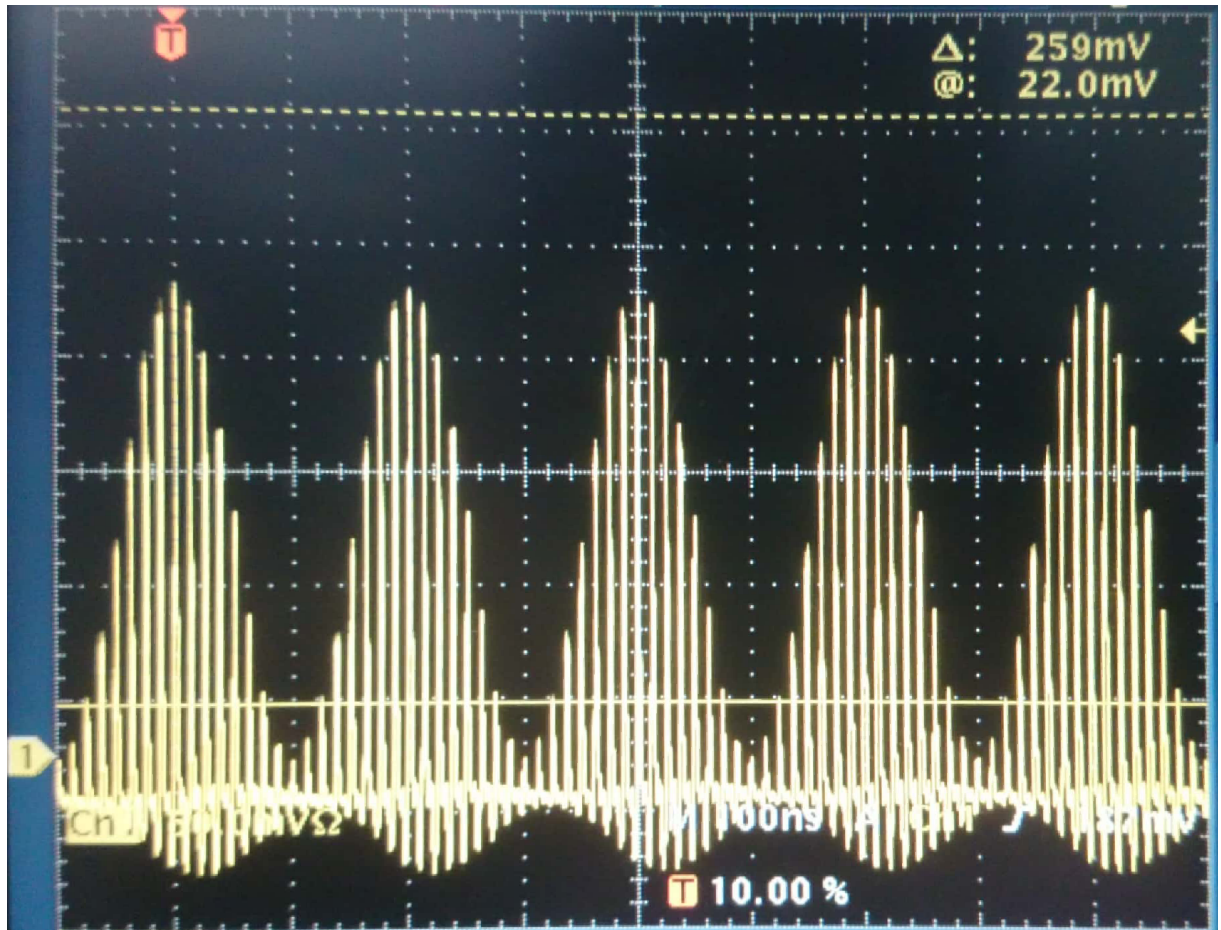


Figure 7: A badly modulated laser beam. 1st order output of the AOM is monitored with a fast photodiode

2.2.2 DC Level Shifter and Synchronous Phase Control

For having the desired modulation phase shift either 90° or 180° between the two pumps we require 2 synchronized function generator in order have control over the phases. With our current equipment, our fist option was using Stanford Research Function Generator and synchronize it with the Sync out put of the SR884 Lock-In Amplifier. The problem is, the output would be in Mega Hz range while the Sync input of the function generator is only in order of 10 KHz. Synchronization in this direction is not possible. Even trying the other direction is hopeless while the accepted

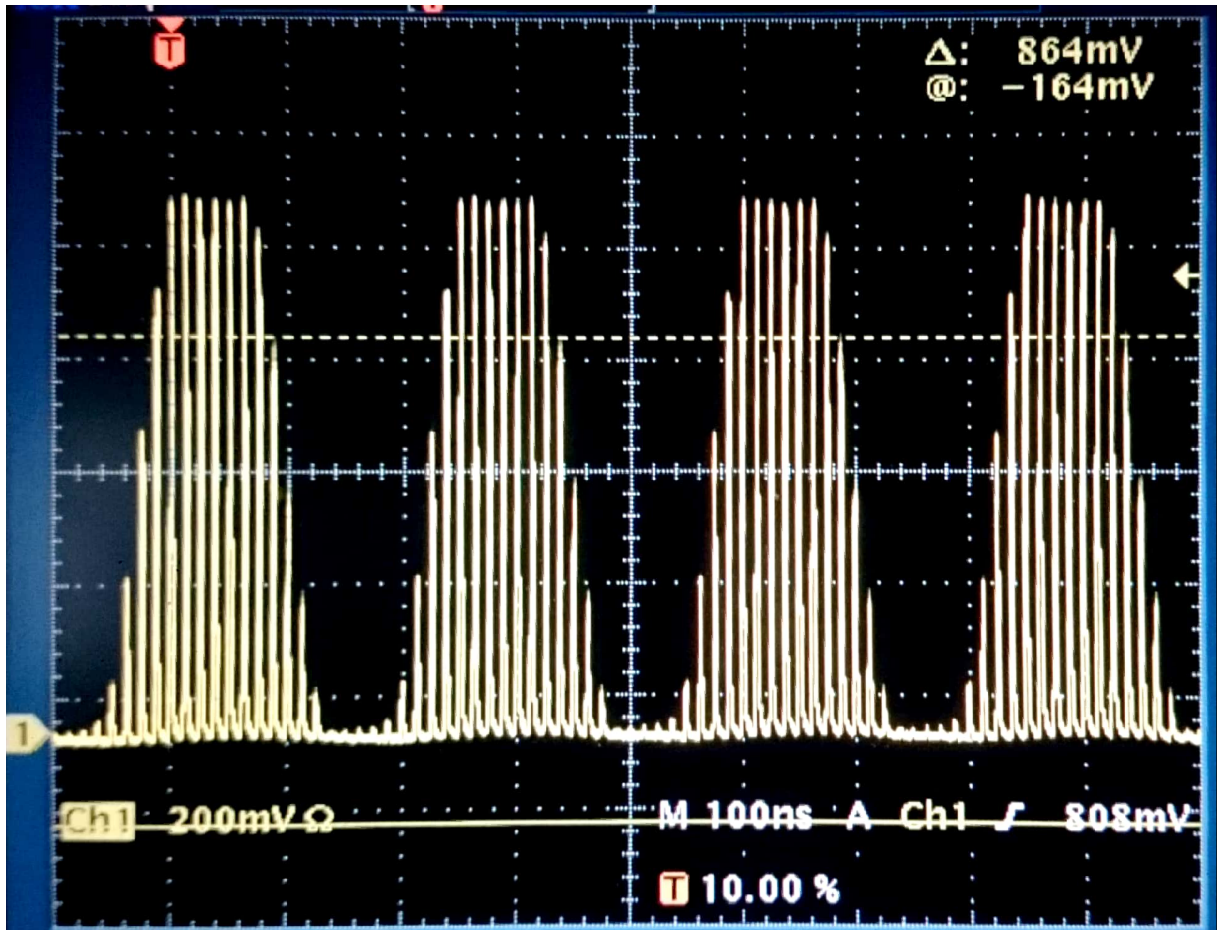
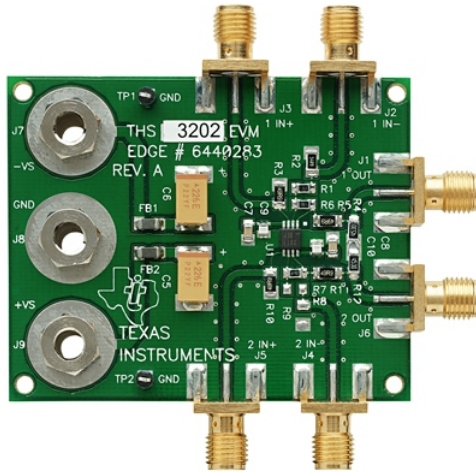


Figure 8: A perfect modulated laser beam. 1st order output of the AOM is monitored with a fast photodiode

sync input range for the lock-in is in order of KHz. Therefore using the lock-in and function generator pair is not considered as an option anymore. The easiest way is, purchasing another function generator which is not very cost-effective and takes some time both of which are not desirable. Eventually, the function generator has another 10 MHz output. The front panel has no control over this output neither its phase nor amplitude. To drive the AOM RF Modulator, the signal should be a square wave from 0-1 v while the 10 MHz output is a sine wave from -0.5-0.5 v. To satisfy our needs we were obliged to build an external module to convert the sine wave to square wave and adjust the amplitude to 0 to 1 v (figure.9) based



Figure 9: The diagram of how the circuit works.



on THS3202EVM³.

To evaluate and fine-tune the required components before ordering the parts, simple simulation has been carried out, figure.9. In THS3202EVM is a double channel 2GHz operational amplifier. The first channel was used to saturate the bias voltage of the op-amp, then the large amplitude is attenuated due to the required large gain to 1 volt and then it is sent to the second channel to add required DC offset. This module enable the setup to reach the highest possible conversion efficiency so the degradation of sample is minimized due to the unmodulated offset.

For optimization purpose, this module has been designed to have control over the amplitude, rise time, duty cycle and DC offset. In addition, we need know that a 50% duty cycle is necessary to drive the AOM, therefore

³The THS3202EVM provides a platform for developing dual amplifier circuits on the same board. The user needs only add power, input signal, and test instruments to operate the EVM. The user can change the feedback and gain resistors to change the gains.

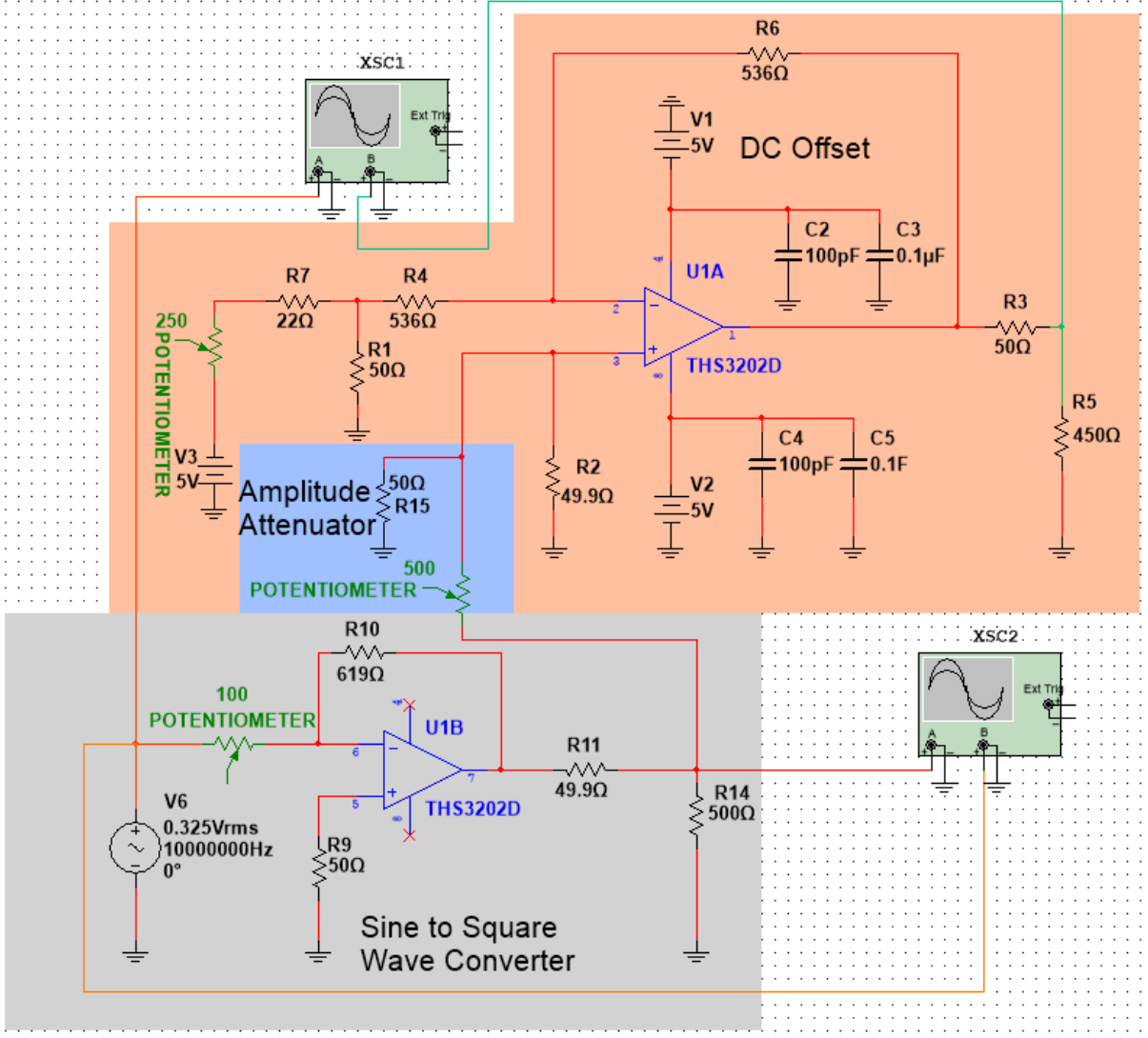


Figure 11: Designed circuit for the sine wave to square wave conversion and DC level shifter.

the intensity distribution over 0th and 1st order is uniform and consistent.

2.2.3 Donut Mode generation and optimization

There are few parameters that can affect the quality of the toroidal intensity distribution. The suitable laser mode for toroidal generation from the vortex phase plate is a Gaussian mode, TEM₀₀. However, this is always not the case the beam profile deviates from Gaussian mode due many to many interaction between the laser beam and the optical elements. I will

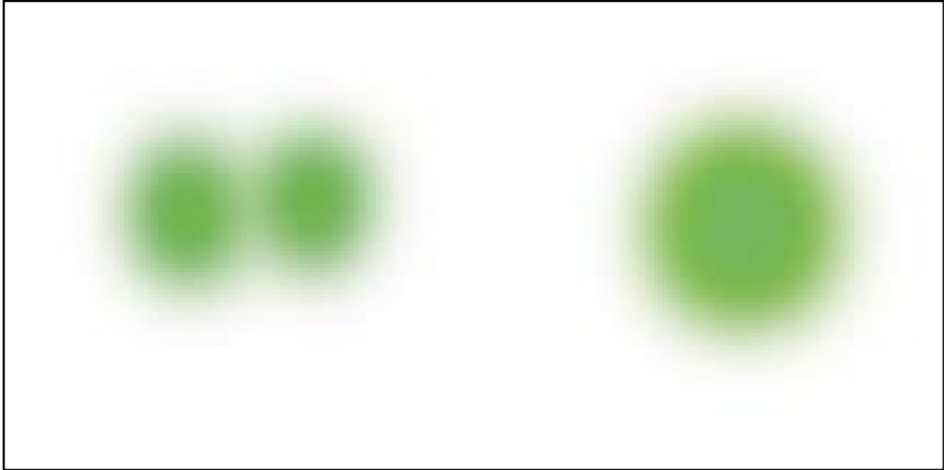


Figure 12: Illustration of beam profile for the 0th and 1st order from left to right respectively. [21]

try to address the most important cases and offer a solution to overcome the beam profile distortion for both the pump and probe beam.

AOM, in fact, has big contribution to beam profile deformation after deflection from the crystal. Even in perfect alignment condition the 0th order output of AOM looks like Figure 12 left and 1st order looks like fig12 right. [21] In practice though, it can be a mix if one does not own a beam profiler to optimize this parameter. To over come this, a presence of a well-optimized spatial filter is crucial to filter other laser mode rather than the Gaussian mode.

Depends on which order is used, one should know that there is more loss in intensity after the spatial filter if the 0th order beam is selected. For our experiment we decided to use the 1st order throught our experiemnt to avoid this distortion, intensity loss after the spatial filter and the lack of unmodulated pulses.

The incident polarization of the beam plays a vital role in the toroidal quality and homogeneous power distribution around the rim and a com-

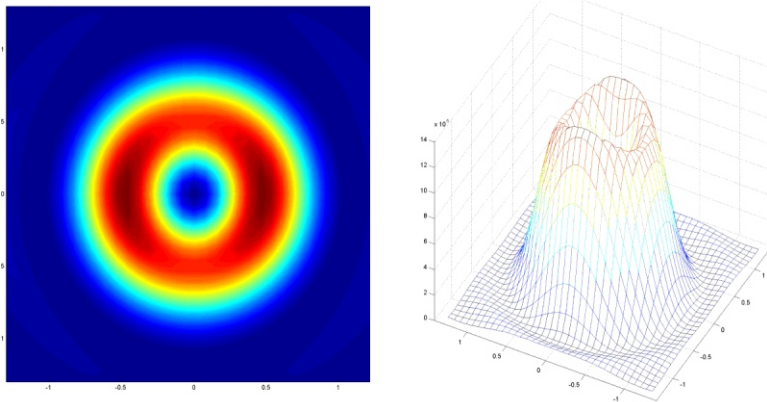


Figure 13: Donut intensity distribution with x polarization results in higher intensity distribution lobes on the left and right

plete destructive superposition at the very center of the toroidal. [22] Studies [23] has revealed its essential role to achieve a smaller particle size and therefore higher resolution. Without the right polarization entering the objective aperture, the power distribution of the toroidal will be more like 2 lobe diagonally through the image while with having a circular polarization we can achieve a well-defined intensity distribution all over the toroidal rim. Having a less perfect toroidal, 2-lobes shape, can deteriorate our effort in resolution enhancement and might cause some diagonally stretched artifacts all over the image. During the system alignment and optimization enough care should be taken to optimize the input polarization of the toroidal. To demonstrate this fact we simulate the toroidal electric field right at the objective focal plane. As it is shown in Figure 13 the toroidal having a x polarization shows a non-uniform power distribution while in Figure 14 uniform power distribution can be observed.

As mentioned theoretically earlier, it can also be observed experimentally that how polarization can affect the quality of intensity distribution

over toroidal. In Figure 15 from left to right polarization varies from 0 (our reference when having the best toroidal), +20, +40, +60 and +80 respectively. This polarization is being controlled by a half-wave plate before the beam enters the galvo scanners and a quarter-wave plate before the objective. At a certain angle the fast axis of the wave plates matches and the beam will have a circular polarization when it enters the objective.

After having the beam mode right and the polarization right, now it comes to perfect alignment of the vortex phase plate (VPP). In our case we purchased the VPP for an array of wavelengths Figure 16. [24] This element enables us to have broader selection for the beam that needs to be shaped in a form of a toroidal mode. Although its versatility of this element, it also imposes a selection of wavelength that can be used with.

To align the VPP, it is important to know the beam should be normal to the surface, the size should fill the phase mask area, polarization should be parallel to the layout. After adjusting the polarization and the size accordingly, to make sure the beam is normal to the surface of the VPP,

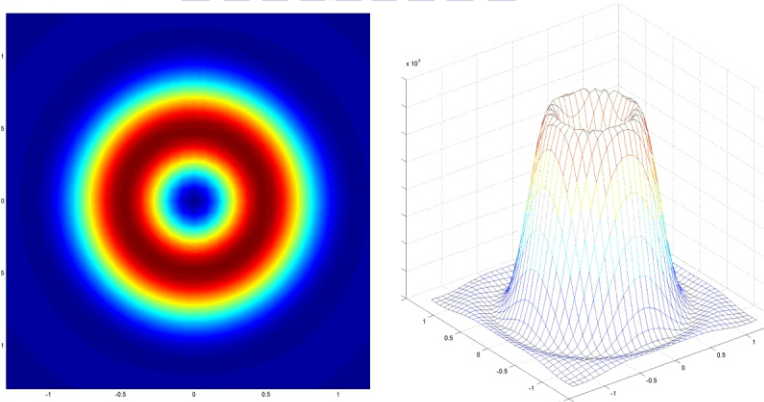


Figure 14: Donut intensity distribution with circular polarization shows a very uniform intensity distribution at the focal plane.

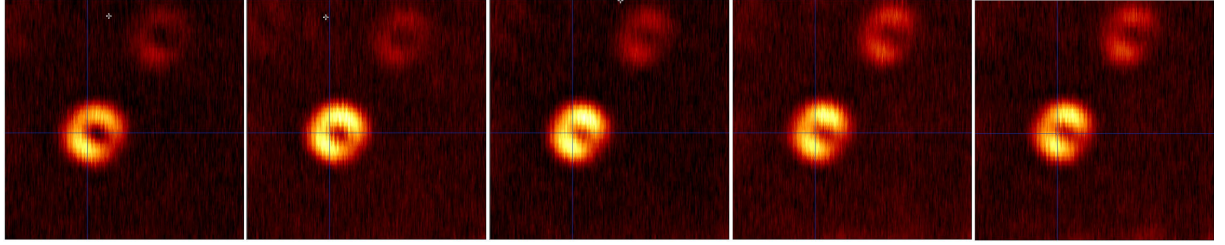


Figure 15: Donut polarization dependence. From left to right the polarization is rotated. This rotation of polarization will cause a circular polarization turn into elliptical. Not having a circular one will result in a less uniform intensity distribution over the toroidal.

some small experiment can be done. Depending on the wavelength, we should image a nanoparticle and by adjusting the tilt angle, x-y translation we can get the optimized toroidal mode.

Another factor that can affect the quality of the toroidal is the phase we select for the lock-in. When the measurement is phase sensitive, it is important to determine the precise value. Shown in Figure 17, when the phase is right, there is a leak to the 90° off of the in-phase channel (quadrature channel). This poor setting will deteriorate the signal acquisition as

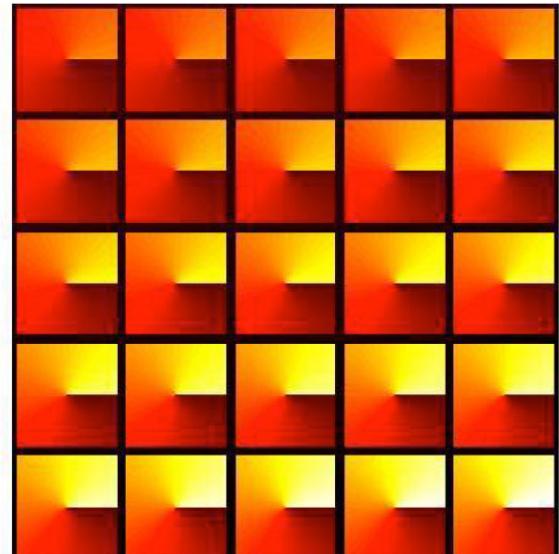
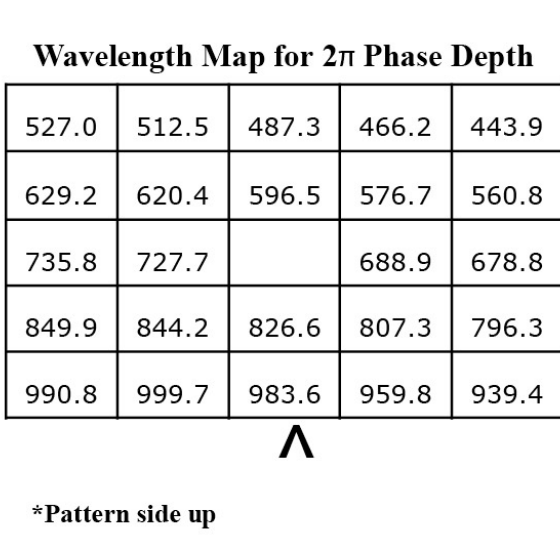


Figure 16: VPP1 vortex phase plate for an array of wavelengths (left) and the phase mask (right)

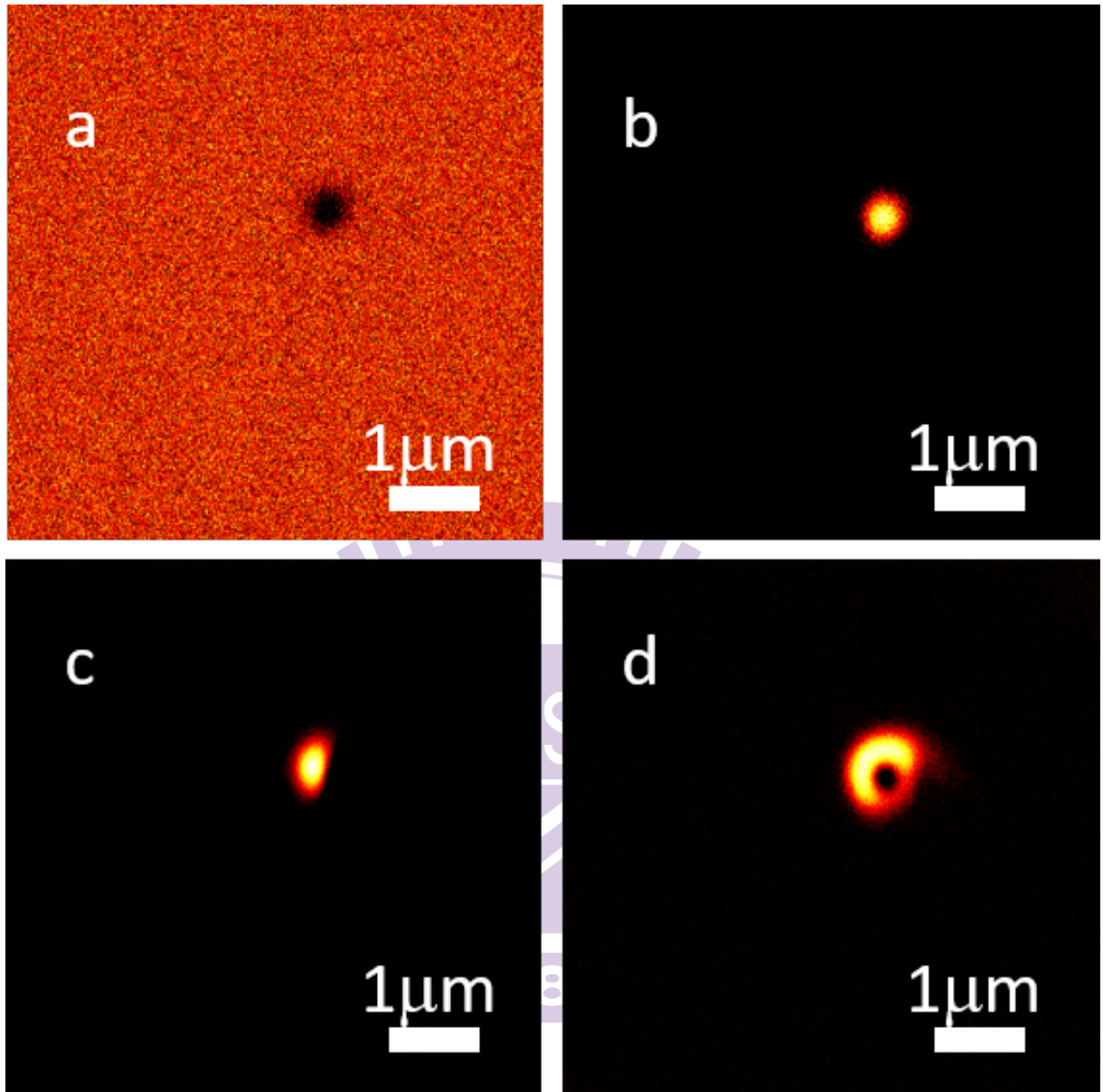


Figure 17: the importance of precise phase selection; a) wrong phase for in a) quadrature b) in-phase channel for gaussian pump beam. Wrong phase for c) quadrature d) in-phase channel for the toroidal beam

we only rely on the in-phase (and out-of-phase) channel.

Once the alignment is done correctly, one should be able to obtain a toroidal mode shown in Figure 18

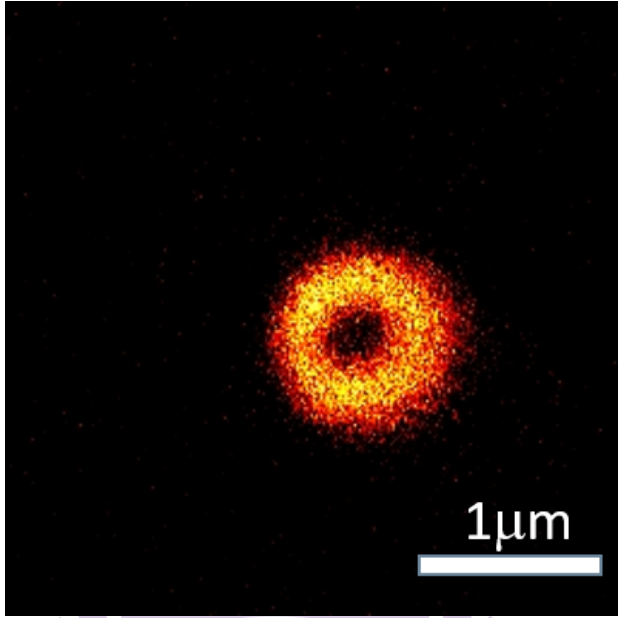


Figure 18: Perfect Doughnut by acquiring thermal lensing effect signal from ZnO nanoparticles pumped only with the toroidal mode beam

2.2.4 Telescope Alignment and Spatial Filter

In this optical layout the beam path from the laser source to the inverted microscope is approximately 130 cm for the pump beams and 200 cm⁴ for the probe beam. Therefore, there is a necessity to have control over the beam size to satisfy the following conditions; a) the back aperture of the objective lens should be over-fill to guarantee uniform excitation within the focused beam area (Figure 19). [25] b) the incident beam on the scanning mirrors are limited and should not exceed 2 mm.

There are 2 types of telescope or expanders in general. In one case, the pair of lens are both positive (convex); this configuration is called Keplerian(Figure 20). Beam size adjustment can also be achieved with a pair of positive (convex) and negative (concave) lens which is called

⁴the extra length is to compensate for the additional paths inside the optical parametric oscillator (OPO)

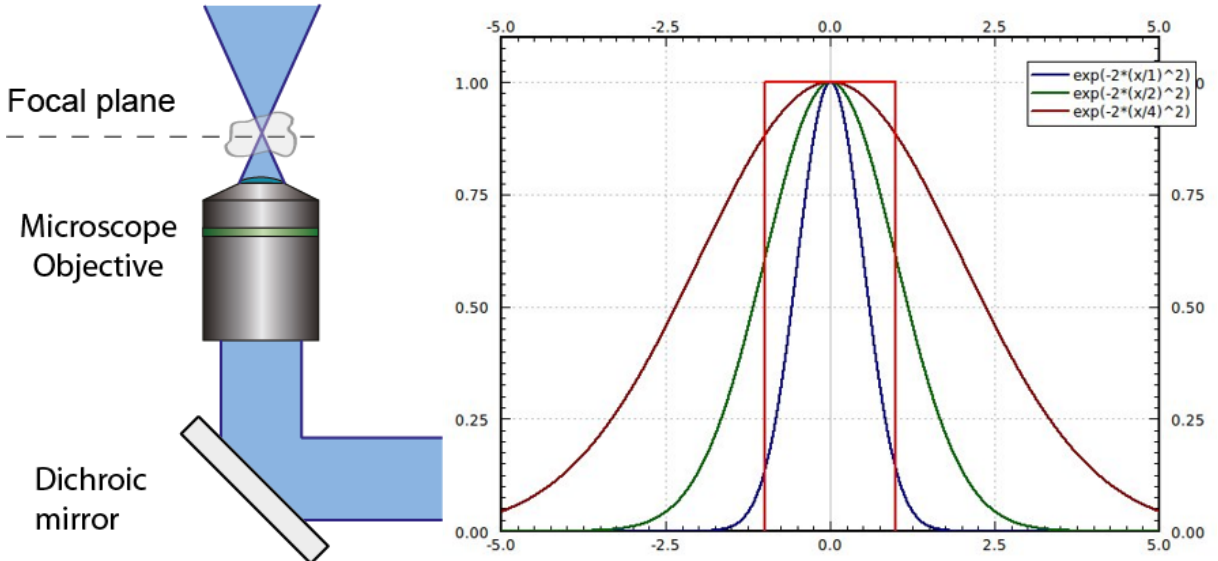


Figure 19: left: schematic of input aperture overfill. right: Objective back aperture entrance is marked with a red rectangle; beam profile with overfill factor 1 (blue), 2 (green) and 4 (dark red). when the objective is not overfilled, the intensity at the edges $\frac{1}{e^2}=0.14$ when it is overfilled by a factor of 2 this is increase to 0.61 of the maximum. [25]

Galillia (Figure 20). In Keplerian configuration we can also filter the beam profile by placing a pinhole at the confocal position. In both configuration the output beam size has the below relationship with the input beamszie and the lens combination:

$$\frac{D_o}{D_i} = \frac{F_o}{F_i} \quad (2)$$

where D_o , D_i , F_o and F_i are output beam diameter, input beam diameter, focal length of the input lens and focal lens of the output lens, respectively.

Although from the equation 2 it can be inferred that the ration of the focal length of the lens combination can be of any value, there are more consideration that needs to be taken. From equation 2 by choosing the ratio between the focal lengths one can shrink or expand the beam size arbitrarily. Accordingly, the expansion ratio affects the divergence parameter of the collimated beam as well. The divergence angle follows the focal

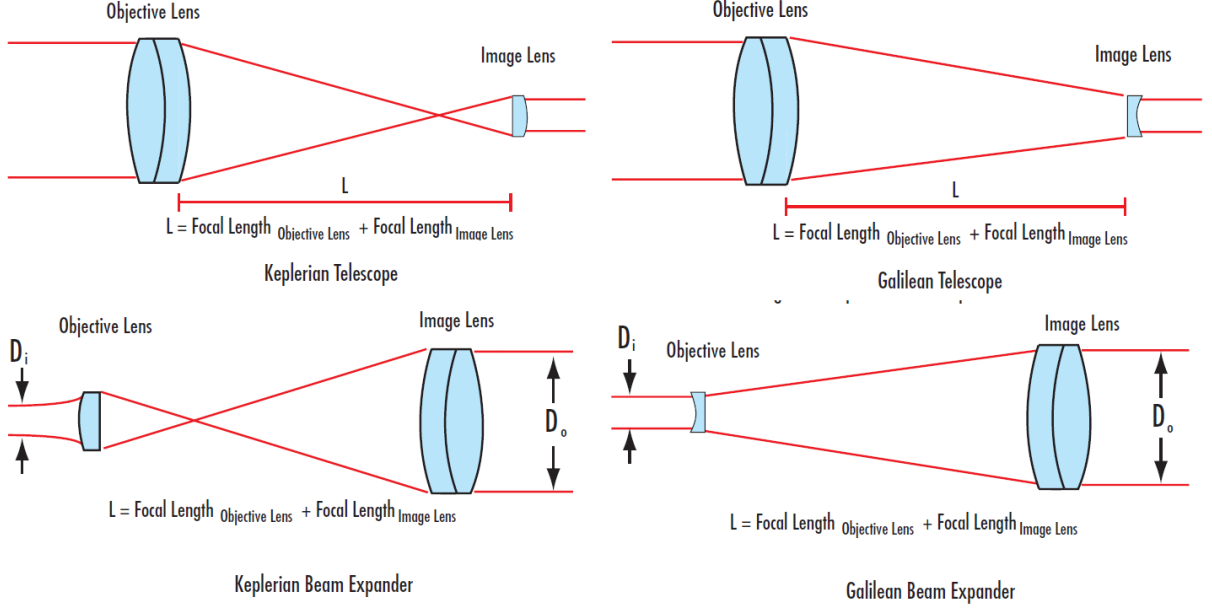


Figure 20: Two different configuration for beam expander and telescope. Keplerian and Galillian. Keplerian configuration consist of two convex lens and Galillian configuration has one convex and one concave lens. Keprian configuration has a real focal place whereas, in Galillian configuration this is imaginary. [26]

length ratio as below:

$$\frac{\theta_o}{\theta_i} = \frac{F_i}{F_o} \quad (3)$$

Where, $\theta_{o,i}$ are divergence angle of the output and input beam respectively. It can be understood that shrinking the beam diameter results in higher divergence angle (and vice versa). Therefore, one must find a right combination for a desired beam path length of the optical layout. Over the whole optical layout of our setup the ratio between the focal lengths did not exceed 3:1(or vice versa) as we experienced large divergence angle. This parameter made the beam size management at the scanning mirros and the back aperture of the objective impossible.

Mentioned earlier in this section, there is need for spatially filter the beam profile to achieve diffraction limited point spread function at the

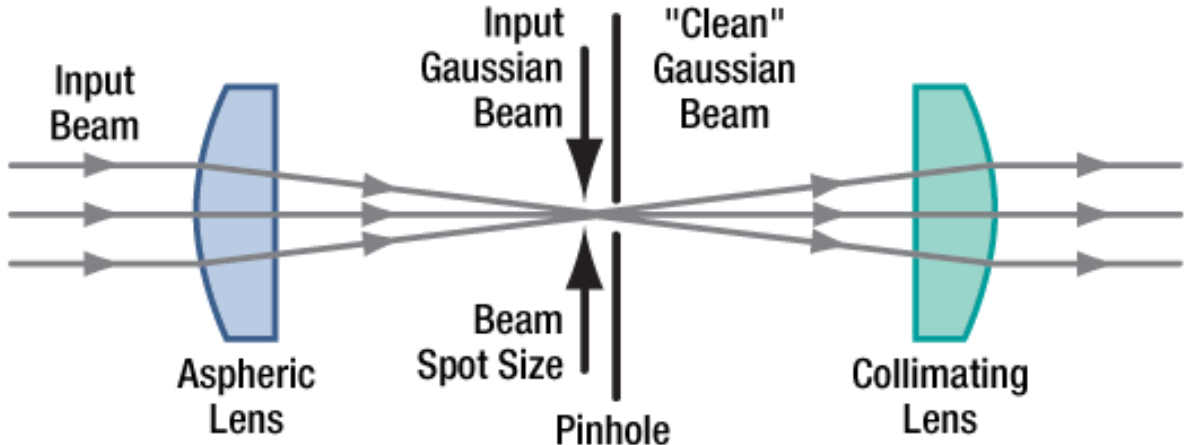


Figure 21: Schematic design of the a spatial filter. [27]

sample and toroidal beam mode with uniform intensity distribution. The spatial filter is a combination of two positive lenses and a pinhole(Figure 21). The beam size at the focal plane is:

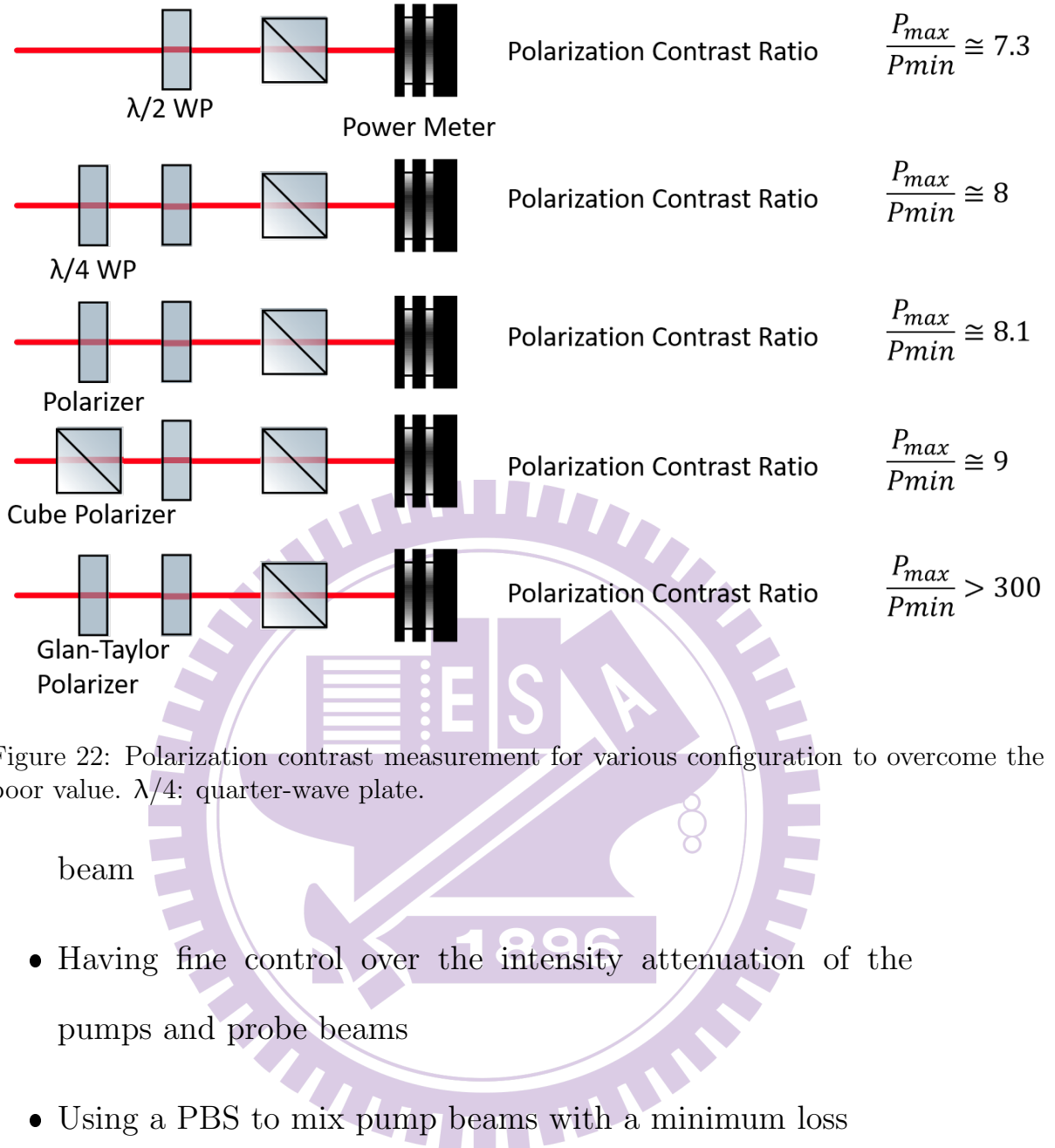
$$D = \frac{\lambda F}{r} \quad (4)$$

Where r is the input beam radius at $1/e^2$ point, λ is wavelength and f is focal length of the used lens. A good approximation recommended by optic manufacturers [27] is to choose a pinhole with the size 30% larger than beam size at the focal plane. This way, is a good trade off to have a lowest effect on intensity loss and good beam profile correction.

2.2.5 Polarization Contrast Measurement and Correction

As Disscussed earlier the polarization is crucial for toroidal mode generation, alignment, attenuation and mixing. Therefore This setup requires a very high polarization contrast over the optical layout for:

- Generating a uniformly intensity distributed toroidal mode



To achieve this we started by measuring the polarization contrast right after the source output. We found out the direct output of the OPO has very poor polarization contrast. the measurement was done as follows. A power meter was placed after output and between them, a polarizer (PBS) before the power meter and half-wave plate ($\lambda/2$) after the output (Figure 22). By adjusting half-wave plate we measure power at its maximum and minimum. The ratio of these two measurements indicates the polar-

ization contrast. This parameter for the direct output of the OPO is (to our surprise) ≈ 7.3 Which is much lower than the official specification of this equipment. This poor contrast ratio could be the result of depolarization, polarization rotation or elliptical polarization conversion⁵. There are various ways to overcome this right after output which will be discussed below.

To evaluate the level of deviation from the linear polarization a quarter-wave plate (λ) was placed after the OPO output(Figure 22). With this element one can compensate for the introduced retardation inside the cavity and recover the linear polarization. Although the polarization contrast improved (≈ 8), it did not result in a significant change. This implies that, there is significant level of depolarization introduced by the cavity. In this situation it is best to filter out the unpolarized light and to have a clean polarized beam. Choosing a polarizer that fits right for this situation is crucial. Three typical polarizer were tested here which is shown in Figure 22 and discussed as follows. A film polarizer is the first element that we tried. Although this element has very height polarization ⁶ contrast ($\approx 10^5$) it has very low damage threshold. [28]. The next option was using a PBS which also was not very successful. PBS has much higher damage threshold compared to film polarizer but it has a poor polarization contract. [29] Finally, we decided to place a Glan-Talor which has a high damage threshold and a height polarization contract. [30] By means of this element the

⁵Some optics could introduce some phase retardation that makes a linearly polarized beam deviates from its linearity to some extent.

⁶The film polarizer was damaged spontaneously so the measurement showed no significant improvement.

polarization contract improved significantly. In fact, there was a large intensity loss more than 30% which is irrelevant for this setup. The main concern here was the pulse stretching after this large optic but as the laser pulse is not close to the transformation limit, the introduced chirping was negligible.

The polarization is now corrected right after the OPO, however there some other context that will affect the polarization linearity and direction drastically. In this setup for two situations it was required to correct and filter the polarization once more to have reliable p-polarized beam over the layout and have fine control with the configured intensity attenuates. As discussed before to matched hight of the beam to the input of the microscope the beam has be lowered by means of two mirrors right out after the OPO. Due to the space restriction the angle of incidence on these two dielectric mirrors are larger than 45° which has additional effect on the polarization. To resolve this the Glan-Taylor polarizer was placed after adjusting the height to compensate for this effect. Another issue that was observed was how the retroreflector affects the polarization. Although the polarization of the incident beam is linear with good approximation but the existing small deviation from this linearity causes complexity in the polarization of the reflected beam. For this case, the depolarization and polarization rotation varied for the incident beam wavelength. To overcome this issue, an additional Glan-Taylor polarizer was placed after the retroreflector to filter the polarization desirably. Keep it mind that, this element should be rotated according to the wavelength.

As a side note, as mentioned in more details above, PBS is used in the intensity attenuators configuration due to its high damage threshold.

2.2.6 Laser Sources

The imaging techniques introduced in this dissertation is based on a Ti:Sapphire (Chameleon Coherent) with 80 MHz repetition rate, a broad tunability (640-1080 nm) and short pulses in order of 140 fs. This laser source is paired with an OPO (Chameleon Compact OPO, Coherent) which can generate femtosecond pulses ranging from 1000 to 1600 nm. This source of laser is very versatile with the combination of the compact OPO. With configuration a broad range linear and nonlinear pump probe microscopy can be done; e.g. two photon fluorescence, SRS, CARS, four-wave mixing (FWM) second harmonic generation (SHG), third harmonic generation (THG), thermal lensing effect and transient absorption imaging.

The use of femtosecond laser give us a better time resolution and a high peak power at low pulse energy which makes the study of nonlinear effect possible. The high repetition rate, although it causes limitation for the measurement time window (12.5 ns in this case) it improves the SNR significantly.

Additionally, with the current technological advancement, there are more and more availability of fiber laser and thin disk lasers out of the industrial application and towards scientific research. Currently, the use of fiber optics has shown great performance in SRS microscopy. [31]. The beam pointing of the fiber laser is stable, it is highly customizable at var-

ious repetition rate, wavelength region and it is maintenance free in long run. Another emerging laser source is the thin disk laser which also can be a good option once it is commercially available. [32]

2.2.7 Galvo-Scanners vs Other Types of Scanners

There are mainly two kinds of scanner that can help to construct image by laser scanning. The device used in our system are a pair of galvo scanners that they change the angle of rotation in respect to the applied voltage. The draw back here lies in the frequency response of the galvo-mirrors. They are designed to work precisely in $\approx 1\text{kHz}$ frequency. Driving them with higher speed results in distortion and blurriness. In a typical xy scanner on axis is called fast axis and the other called slow axis when raster scanning. It is so, as one axis is following the voltage ramp with sampling rate of the source and the other axis only steps down (up) at the end of each ramp. The slow axis does not suffer from image distortion.

One solution to overcome this was introduction of resonant scanners. These devices are hexagonal mirrors that spin at constant frequency, therefore offer a faster acquisition speed. [33] Despite this advantage, there are some limitations in using a resonant scanner (such as nonlinearity) and the it cannot be driven to make costume patterns. Therefore, we proceed to use the galvo-scanner pair and tried to improve the acquisition speed in the labview program and image construction algorithm.

Finally to make sure that the field of view (FOV) is behaving as expected with the zoom level, the microscope should be calibrated with the micro-

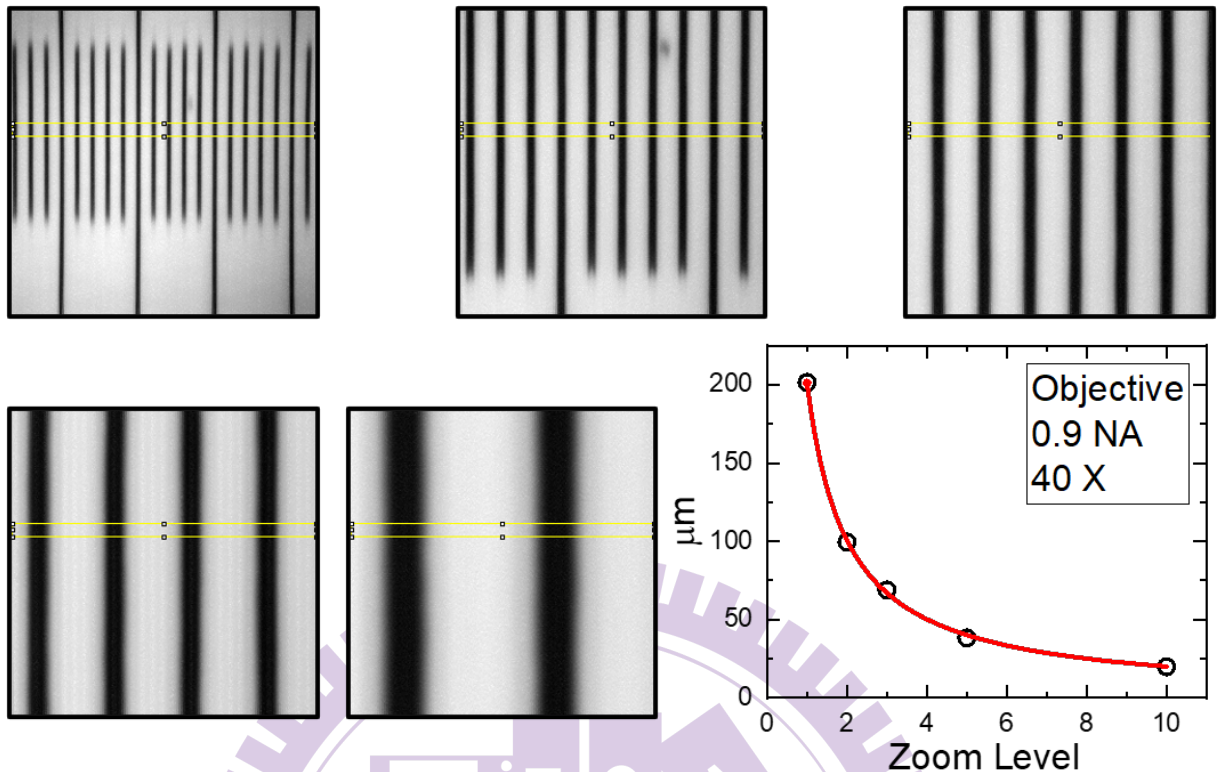


Figure 23: The xaxis is the zoom level (galvo voltage divider) and y-axis the FOV

ruler 23. the relationship between the FOV size and Zoom level should follow $FOVsize \propto \frac{1}{ZoomLevel}$; The zoom level is the value by which the driving voltage applied to the galvo scanners are divided.

2.3 Detection Scheme and Image Acquisition

In this section the types of detection scheme will be discussed briefly and compared with conventional types. A detection scheme is how a certain signal or phenomenon is converted to voltage so it can be digitized and recorded in a computer. Two main scheme that will be our main focus are homodyne and heterodyne detection scheme. In later one, the signal should be modulated at a reference frequency and special equipment is required to demodulate the signal. The detection is achieved through several pho-

Table 1: Comparison between PMT, Photodiode and APD. [34]

Characteristic	PMT	Photodiode	APD
Spectral Coverage (nm)	115-1700	190-13000	190-1700
Peak QE (η) (%)	<40	<90	<90
Active area [mm ²]	12000	100	100
Gain (μ)	$10^5 - 10^6$	1	<100
NEP ^a (W/ $\sqrt{\text{Hz}}$)	$>2 \times 10^{-17}$	$>6 \times 10^{-16}$	$>1 \times 10^{-15}$
Rise Time (ns)	>0.15	>0.23	>0.35
Bandwidth	$<2 \times 10^9$	$<1.5 \times 10^9$	$<1 \times 10^9$

^aNoise equivalent Power. $NEP = \frac{Incident\ Energy \times Area}{\frac{S}{N} \times \sqrt{\Delta f}}$

tosensitive detectors, such as, photodiode, avalanche photodiode (APD) or photomultiplier tube (PMT). These detectors have specific characteristics, such as bandwidth, rise time, sensitivity range and etc, that makes them an appropriate choice for certain applications.

2.3.1 Detector Selection Guide

When building a laser scanning microscope one crucial decision to make during the purchase process is what detector to choose which depends on various parameters depending on the detection scheme, the wavelength region and the time scale of the detection phenomenon. After the decision is made for what sort of signal is being detected and how, then by review a datasheets the final decision is made but there are some guidelines to selecting a detector that will be discussed briefly below for photodiode, APD and PMT.

photomultiplier tube (PMT); the working principle of this device can be found extensively over the web and books, however a typical PMT has the following characteristics in general. It is a vacuum tube that a high

voltage is applied across multiple metal plates (anodes) which can help to amplify a signal in order of 10^5 - 10^6 times. After a secondary electron is emitted by the incident photon, it is accelerated in the electric field and the current amplified in the tube. Therefore, it can be thought that PMT is a current source which is capable of detecting a single photon. Summarized in table 1, it can be inferred, this detector is fast (100s of picoseconds) and it is perfect for visible region. For near infra red (NIR) region, it needs water cooling and the gain is not very high. Sensitivity wise, nothing is compared with PMT in general.

Photodiode; This detector is a current source as well as it absorbs photons generated photocurrent but there is no gain or amplification intrinsically. The current to voltage converter is connected in general application or it is the detector is mounted on it. Generally, there is preamplifier which is transimpedance amplifier or in other words a current amplifier and the voltage amplifier is setup as a next stage to obtain acceptable SNR. Photodiode is an appropriate choice for visible and NIR region. This detector, depending on the material (silicon, germanium, etc) can reach wavelengths of 13000 nm. Having that in mind, the response time here, depends on the active area and circuit that the semiconductor is connected to. To reach under nanosecond rise time the active area should be below 1 mm^2 . The rise time depends on the coupling circuit.

$$f_{BW} = \frac{1}{2\pi R_L C_J}, t_R = \frac{0.35}{f_{BW}}$$

Where f_{BW} , R_L , C_J and t_R are frequency band width, load resistance, diode capacitance and rise time, respectively.

avalanche photodiode (APD); These class off detectors are semiconductor based but are driven in avalanche mode; a reverse biased is applied across the bandgap which makes the avalanche behavior through impact ionization phenomena after an incident photon. Therefore, the response is not linear but the rise time is shorter compared to photodiode and gain is higher significantly. Although it is not as sensitive as a PMT, this detector can be an appropriate choice for NIR as well without cooling. One drawback in this class, is their rather small active area which limits the design and makes the alignment more critical.

In the design of this pump-probe microscope for SRS, thermal lensing effect and transient absorption microscopy, photodiode was used as the probe is close to NIR region and the detection scheme is heterodyne - further discussion in the next section. In case of CARS microscopy, PMT was used as the anti-stoke signal is in visible region. For latter case, as it is background free the signal was directly (without using lock-in amplifier) acquired after rectification.

2.3.2 Heterodyne and Homodyne detection scheme

As mentioned earlier, for probing different phenomena certain detection scheme was required. Detection scheme refers to how the signal is acquired and separated from the background or noise. If the probing (detected) wavelength varies from the source of excitation (the incident beam), the

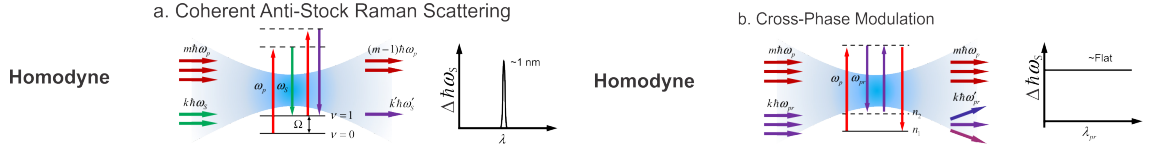


Figure 24: Microscopy techniques that can be detected in homodyne scheme.

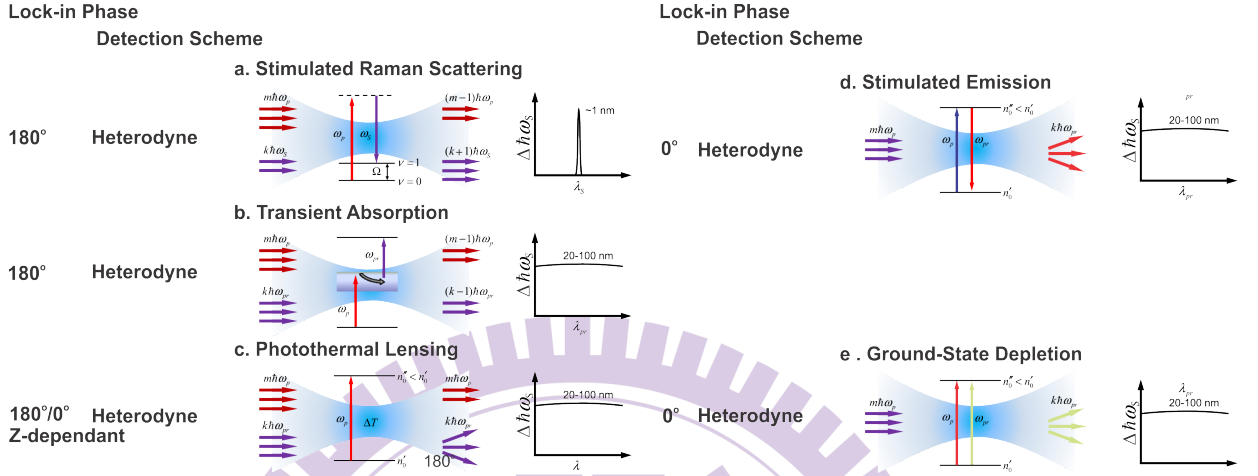


Figure 25: The microscopy technique that within the heterodyne detection scheme with their detected phase in respect to the pump modulation.

detection is homodyne. Although it is counterintuitive, it is rather important to know that the frequency of the incident beam and the detected beam are the same, hence the prefix homo-. For example cross-phase modulation (XPM) and CARS microscopy technique (Fig. 24) are as within this scheme. [35] In this classification the signal intensity is proportional to the E^2 . In contrast, if the detected wavelength is identical with any of the incident beam (E_{in}) then the signal intensity is proportional to $|E+E_{in}|^2$, this term is why phenomenon as such are classified under heterodyne scheme. [36] In this scheme a usage of a lock-in amplifier is necessary to separate and demodulate the signal from background. Such techniques are, SRS, TA, photothermal lensing, stimulated emission and ground-state depletion microscopy (Fig. 25). [35]

2.4 Pump-Probe Microscope Graphical User Interface

To comply with our needs and provide us with enough flexibility we wrote a customized graphical user interface by using National Instrument data acquisition board. The GUI, figure.26 can control the Galvo scanners and collect pixel value at each step. The voltage ramp sent to the galvo scanners gives us enough flexibility to rotate or move our field of view while we are at higher zoom level. It also can perform time resolved experiment.

Different part of the LabVIEW program is explained as following

- a. Voltage ramp control to offset the scanning in x-y direction for tracking a particle or fine-tuning the region of interest (ROI). This part has also control over the rotation of the raster scanning for aligning the image in the FOV
- b. Scanning mode; This program is designed to do raster scanning, scanning a square of the desired FOV and deriving the mirror to any arbitrary binary image. The arbitrary pattern does scale with the zoom level.
- c. Zoom Level; which adjust maximum and minimum voltage applied to the mirrors.
- d. Realtime or averaged mode selection
- e. Resolution selection; it can select between 128, 256, 512 or 1024 pixels.

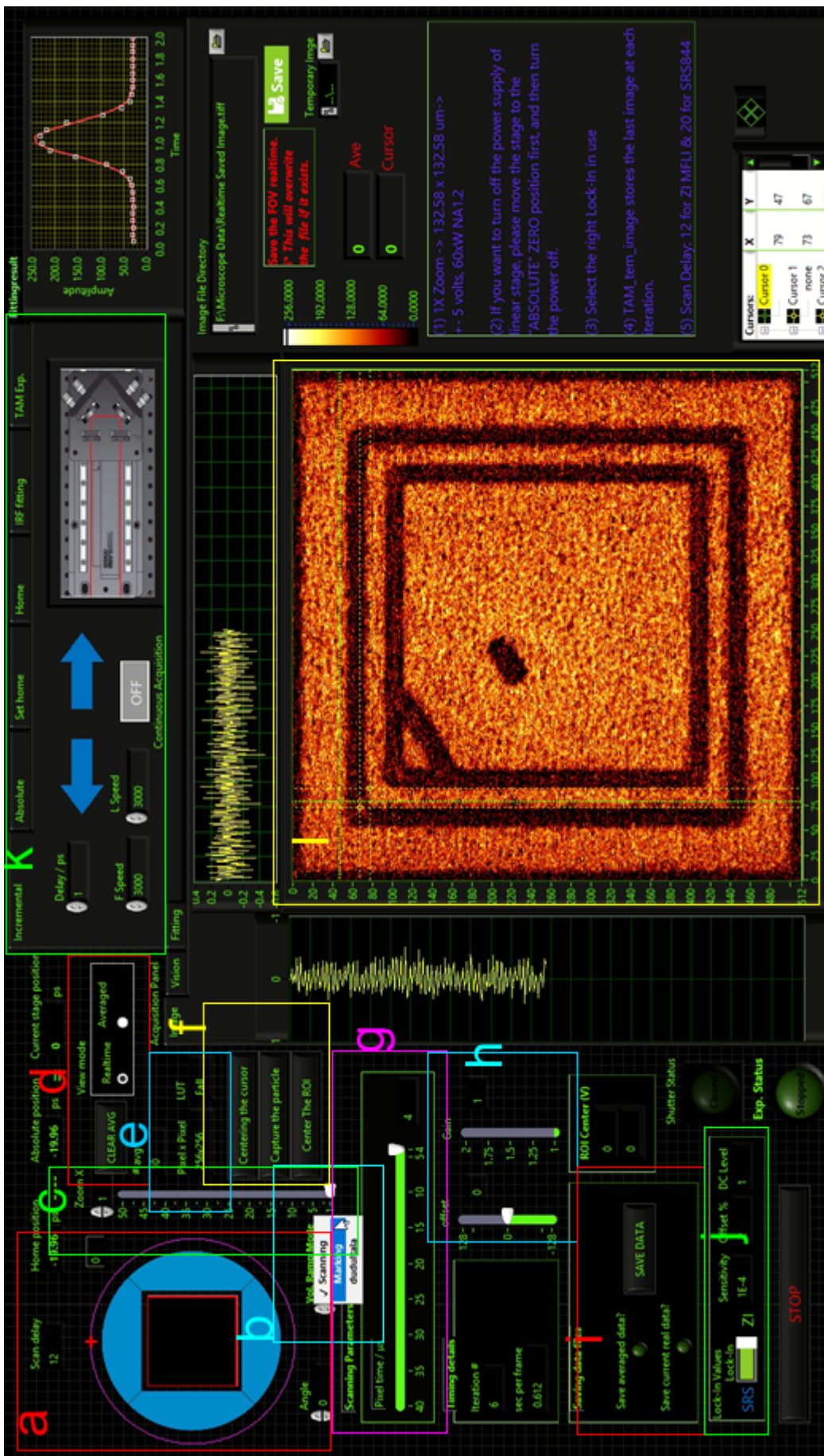


Figure 26: GUI of the home writing labview program to perform time resolved pump-probe microscopy

- f. Capturing a particle, resetting the FOV and centering the cursor.
- g. Scan speed; which can select from $4\mu\text{s}$ to $40 \mu\text{s}$.
- h. Adjusting the offset and gain for the realtime image.
- i. Saving the image as raw text file.
- j. Lock-in Selection; this can select between Zurich Instrument MFLI (or any other model) and Stanford Instrument SR844.
- k. Delay line control and transient pump-probe measurement setup.
- l. Image view.

